0.4 e $Å^{-3}$ theory), lone pairs (0.4 and 0.5 e $Å^{-3}$), holes behind the S—O bonds (−0.3 and −0.4 e $Å^{-3}$). However, in addition, there are differences around the sulfur atoms. The experiment shows a ring of excess density, peaking in the S—O bond and behind it, which does not appear in the theory. While, as previously mentioned, the double nature of the peak of the S—O bond may be an artefact of the modelling, the feature of a rather flat maximum, stretching close to the sulfur site is real and is clearly different from theory. The theoretical treatment does not contain polarization functions of f symmetry in the sulfur atom. An f_{xyz} orbital would be required to generate the peak which is observed.

A more detailed comparison of experiment and theory must be made directly between the observed, thermally smeared, deformation density and similarly treated theoretical densities, rather than attempting to remove thermal motion from the experiment by this model-dependent method. In a subsequent paper we shall attempt this.

BNF and PAR are grateful to the Australian Research Council for financial support.

References

BECKER, P. J. & COPPENS, P. (1974). *Acta Cryst.* A**30**, 129–147.

CHANDLER, G. S., CHRISTOS, G. A., FIGGIS, B. N. & REYNOLDS, P. A. (1992). *J. Chem. Soc. Faraday Trans.* 2, **88**, 1961–1969.

CLEMENTI, E. & ROETTI, C. (1974). *At. Data Nucl. Data Tables*, **14**, 177–478.

CONDON, E. V. & SHORTLEY, G. H. (1957). *The Theory of Atomic Spectra*, pp. 158–186. Cambridge Univ. Press.

COPPENS, P., GURU-ROW, T. N., LEUNG, P., STEVENS, E. D., BECKER, P. & YANG, Y. W. (1979). *Acta Cryst.* A**35**, 63–72.

COPPENS, P., LEISEROWITZ, L. & RABINOVICH, D. (1965). *Acta Cryst.* **18**, 1035–1038.

CROMER, D. T. & LIBERMAN, D. (1970). *J. Chem. Phys.* **53**, 1891–1898.

FIGGIS, B. N., KHOR, L., KUCHARSKI, E. S. & REYNOLDS, P. A. (1992). *Acta Cryst.* B**48**, 144–151.

FIGGIS, B. N., KUCHARSKI, E. S. & REYNOLDS, P. A. (1989). *Acta Cryst.* B**45**, 232–240.

FIGGIS, B. N., REYNOLDS, P. A. & WHITE, A. H. (1987). *J. Chem. Soc. Dalton Trans.* pp. 1737–1745.

FIGGIS, B. N., REYNOLDS, P. A. & WILLIAMS, G. A. (1980). *J. Chem. Soc. Dalton Trans.* pp. 2339–2347.

FIGGIS, B. N., REYNOLDS, P. A. & WRIGHT, S. (1983). *J. Am. Chem. Soc.* **105**, 434–440.

HENRIKSEN, K., LARSEN, F. K. & RASMUSSEN, S. E. (1986). *J. Appl. Cryst.* **19**, 390–394.

HERMANNSON, K. (1984). Doctoral Thesis, Univ. of Uppsala, Sweden.

IVERSEN, B. B., LARSEN, F. K., FIGGIS, B. N. & REYNOLDS, P. A. (1993). *Acta Cryst.* B**49**. In preparation.

KISSEL, L. & PRATT, R. H. (1990). *Acta Cryst.* A**46**, 170–175.

LEHMANN, M. S. & LARSEN, F. K. (1974). *Acta Cryst.* A**30**, 580–584.

LE PAGE, Y. & GABE, L. J. (1979). *Acta Cryst.* A**35**, 73–78.

MABBS, F. E. & PORTER, J. K. (1973). *J. Inorg. Nucl. Chem.* **35**, 3219–3222.

REYNOLDS, P. A., FIGGIS, B. N., KUCHARSKI, E. S. & MASON, S. A. (1991). *Acta Cryst.* B**47**, 899–904.

STEWART, R. F., DAVIDSON, E. R. & SIMPSON, W. T. (1965). *J. Chem. Phys.* **42**, 3175–3187.

VARGHESE, J. N. & MASON, R. (1980). *Proc. R. Soc. London Ser. A*, **372**, 1–7.

WEISS, R. J. & FREEMAN, R. J. (1959). *J. Phys. Chem. Solids*, **10**, 147–161.

Acta Cryst. (1993). B**49**, 806–811

Electron-Density Distribution in a Crystal of Dipotassium Tetrafluoronickelate, K_2NiF_4

BY S. K. YEH, S. Y. WU, C. S. LEE AND YU WANG*

Department of Chemistry, National Taiwan University, Taipei, Taiwan

(*Received* 15 *December* 1992; *accepted* 29 *March* 1993)

Abstract

Dipotassium tetrafluoronickelate(II), K_2NiF_4, M_r = 212.90, tetragonal, $I4/mmm$, a = 4.0130 (6), c = 13.088 (2) Å, V = 210.78 (4) $Å^3$, Z = 2, T = 300 K, D_x = 3.36 Mg m^{-3}, Mo $K\alpha$, λ = 0.7107 Å, μ = 656 mm^{-1}, $F(000)$ = 204, final R = 0.018 for 698 unique reflections [$I > 2\sigma(I)$]. Charge asphericity around the Ni atom caused by the splitting of 3d orbitals is clearly observed in the deformation density. Although the exact site symmetry at the Ni atom is D_{4h}, the local geometry around Ni is practically O_h with Ni—F distances of 2.0065 (3) and 2.0062 (8) Å. The d-orbital occupancies derived from the multipole coefficients are in accordance with the prediction of simple crystal-field theory. The splitting of the d orbitals in D_{4h} is e_g, b_{2g} (from t_{2g} orbitals in O_h), and b_{1g} (from e_g in O_h). The occupancies of all these orbitals are nearly equal with e_g the largest (1.57), b_{1g} and b_{2g} the second largest (1.54), and a_{1g}

* To whom all correspondence should be addressed.

the smallest (1.51). Although the differences in occupancies are small, asphericity around Ni can be observed in the deformation-density distribution. Positive deformation density corresponding to e_g (d_{xz}, d_{yz}) orbitals, negative troughs corresponding to an a_{1g} (d_{z^2}) orbital and slightly negative density corresponding to b_{1g} ($d_{x^2-y^2}$) and b_{2g} (d_{xy}) orbitals are manifested around the Ni atom.

Introduction

Two potassium nickel fluorides $KNiF_3$ and K_2NiF_4 have been identified in the KF–NiF_2 binary system (Wagner & Von Balz, 1952). The former compound has a standard perovskite structure. The latter was found to be tetragonal (Von Balz & Plieth, 1955). Both are antiferromagnetic (Von Rüdorff, Kändler & Babel, 1962). The magnetism of K_2NiF_4 has been studied both experimentally (Birgeneau, Guggenheim & Shirane, 1969; Plumier, 1964) and theoretically (Kobler, Eyert & Sticht, 1988). The optical properties of K_2NiF_4 have also been investigated extensively (Abdalian & Moch, 1978; Pisarev, Karamyan, Nesterova & Syrnikov, 1973; Strobel & Geick, 1982; Samoggia, Parmigiani & Leccabue, 1985) and the IR and Raman spectra of this compound indicate symmetry lower than O_h. Although the crystal structure has been known since 1955 (Balz & Plieth, 1955), no accurate atomic parameters have been reported. Since K_2NiF_4 defines an important structure type for many oxides (Singh, Ganguly & Goodenough, 1984), we consider it is of value to determine the structural parameters accurately, while studying the electron-density distribution around the Ni atom. The environment of the Ni atom in the crystal is pseudo-octahedral. The electronic transition of $^3A_2$ to $^3T_1$ and $^3T_2$ states yields a crystal-field splitting energy of $D_q = 800\ cm^{-1}$ and Racah parameters $B = 935\ cm^{-1}$, $C = 3651\ cm^{-1}$ (Pisarev, Karamyan, Nesterova & Syrnikov, 1973). As the exact site symmetry of Ni is D_{4h} (4/*mmm*), we would like to see whether the electron-density distribution around Ni reflects symmetry lowering from O_h ($m\bar{3}m$). Hopefully, the *d*-orbital populations can be further derived from the multipole coefficients and the results compared with the predictions of crystal-field theory.

Experimental

Data collection

The K_2NiF_4 crystal was prepared by comelting KF, NiF_2 and KHF_2 according to methods in the literature (Wanklyn, 1975). A yellowish green crystal with a nice cubic shape was chosen for an accurate electron-density study. Intensity data were collected on an Enraf–Nonius CAD-4 diffractometer using Mo $K\alpha$ radiation at room temperature. Experimental details are given in Table 1. Lattice parameters were obtained by least-squares refinement on 25 reflections in the 2θ range 37 to 95°. Intensity data for a half sphere up to a 2θ of 150° were measured using $\theta/2\theta$ scans. In addition, six equivalent reflections with azimuth angles $\psi = \pm 5, \pm 15, \pm 25°$, for each unique reflection ($+h, +k, +l$; $h > k$) up to a 2θ of 90° were collected. A total of 5651 reflections were measured and corrected for absorption (Alcock, 1969), Lorentz and polarization effects. Three standard reflections were monitored throughout the measurement, the variations all being within ±1%. Three reflections were chosen for detailed study by measuring ψ curves, the agreement between the calculated absorption curve and the measured intensity curve was excellent. The data set consisted of 703 unique reflections after averaging all the equivalent reflections. The interset agreement is 1.7%.

Table 1. *Crystal data of* K_2NiF_4

Crystal system	Tetragonal
Space group	*I*4/*mmm*
Formula	K_2NiF_4
M_r	212.90
a (Å)	4.0130 (6)
c (Å)	13.088 (2)
V (Å^3)	210.78 (4)
Z	2
D_x (g cm^{-3})	3.355
$F(000)$	204
$2\theta_{max}$ (°)	150
Total No. of measurements	5651
Range of h, k, l	h 0–10; k 0–7; l 0–35
R_i*	0.017
λ(Mo $K\alpha$) (Å)	0.71069
Crystal size (mm)	0.3 × 0.2 × 0.3
μ (cm^{-1})	65.6
Transmission range	0.158–0.365
No. of variables	13
R, wR	0.018, 0.020
$(\Delta/\sigma)_{max}$	0.003

* $R_i = \sum|I_i - \bar{I}|/\sum I_i$.

Refinement

The structure was refined by conventional full-matrix least-squares processes both on the full data and on high-order data with $(\sin\theta)/\lambda > 0.85$ Å^{-1}. The function $\sum w(F_o - F_c)^2$ was minimized; $w = 1/\sigma^2(F_o)$ with $\sigma^2(F_o)$ from counting statistics taken from the geometric mean of the equivalents. Atomic scattering factors were taken from the analytical expression in *International Tables for X-ray Crystallography* (1974, Vol. IV). An isotropic secondary-extinction correction (Larson, 1970) was included in the refinement. The program used for refinement was *NRCVAX* (Gabe, Le Page, Charland, Lee & White, 1989).

In addition, multipole refinement was performed with the *MOLLY* program (Hansen & Coppens, 1978). Multipoles were introduced up to hexadecapole level for the Ni and F atoms. The radial functions are $r^{n_l}\exp(-\xi_l r)$ with $n_l = 4$ for all l values on

Ni; $n_l = 2$ for $l = 0, 1, 2$; $n_l = 3$ and 4, respectively, for $l = 3$ and 4 on F, ξ_1 values are 9.239, 5.114 a.u.$^{-1}$ for Ni and F atoms, respectively. The core and valence scattering factors for K, Ni and F atoms were taken from *International Tables for X-ray Crystallography* (1974, Vol. IV). The core-electron configurations were assumed to be He for F, an Ar core for K and for Ni where $4s^2$ was not included, and a Ca core for Ni where $4s^2$ was included. The charge of the crystal was constrained to neutrality with the charge for K at +1. The K^+ ion was taken as spherical since there is no valence electron. Ni, F(1) and F(2) atoms lie on special positions with site symmetries 4/*mmm*, *mmm* and 4*mm*, respectively. The number of multipole parameters is 4, 4 and 6, respectively. The radial parameter, κ, for K is fixed at 1.0. Those for Ni and F were refined. Two parallel refinements, one with $3d^8$ (Ca core) as the valence electron, the other with $3d^{10}$ (Ar core) as the valence electron, were performed. An isotropic extinction correction (Becker & Coppens, 1974)* was also included in this refinement.

Deformation-density maps

Three types of deformation-density maps are presented in this work: The first is the experimentral $\Delta\rho_{x-x}$, where Fourier coefficients are obtained from the difference between F_{obs} and F_{cal} calculated from the high-order [$(\sin\theta)/\lambda > 0.85$ Å^{-1}] refinement. The second is a model deformation-density map $\Delta\rho_{m-a}$ derived from a multipole model where Fourier coefficients are the difference between two F_{cal} values – one derived from a multipole model with a series expansion of spherical harmonics (Hansen & Coppens, 1978), the other being the spherical part of the model density. The third is a static model ($\Delta\rho_{m-a,\,static}$) which is obtained the same way as the aforementioned model density except that all nuclear vibrations are excluded from the calculation and the Fourier summation is extended to the limiting sphere of the radiation (1.41 Å^{-1}).

Results and discussion

The well known crystal structure of K_2NiF_4 is shown in Fig. 1. The perovskite structure unit is still maintained in the crystal, but in the packing each unit is shifted by $\langle\frac{111}{222}\rangle$ with respect to its neighbours. Although the site symmetry around Ni is D_{4h} (4/*mmm*), the six NiF distances [2.0065 (3), 2.0062 (8) Å] are essentially the same and equal to that [2.0057 (4) Å] of $KNiF_3$ (Kijma, Tanaka & Marumo, 1983). Thus from geometric considerations, the Ni atom has pseudo-O_h ($m\bar{3}m$) site symmetry. However, the electron deformation density distribution indicates that the pseudo-O_h symmetry does not persist at a detailed level.

Agreement indices for full-matrix least-squares refinements based on the full data, high-order data, and for the multipole model (d^8) are listed in Table 2.* Positional and thermal parameters obtained from the conventional and multipole refinements (d^8) are given in Table 3. Basically the positional parameters are the same (within 2σ) for all the refinement results. The results from the two multipole refinements with d^8 and d^{10} are essentially the same, only one result is presented.

The deformation-density maps ($\Delta\rho$) containing NiF_4 with fourfold symmetry are shown in Fig. 2. This shows the *ab* plane with $z = 0$ or $\frac{1}{2}$ in the unit cell. The $\Delta\rho$ for the *ac* plane through Ni is presented in Fig. 3, where $\langle 100\rangle$ denotes the horizontal axis and $\langle 001\rangle$ denotes the vertical axis. There is only *mm* symmetry on this plane. Fig. 4 shows the plane that bisects the γ angle, with the $\langle 110\rangle$ vector in the horizontal direction and the $\langle 001\rangle$ vector vertical. Fig. 5 shows the plane bisecting the β angle with $\langle 103\rangle$ horizontal and $\langle 010\rangle$ vertical. In each figure, there are three $\Delta\rho$ maps obtained from (*a*) conventional deformation, $\Delta\rho_{x-x}$; (*b*) multipole-model deformation $\Delta\rho_{m-a}$ and (*c*) static multipole-model deformation $\Delta\rho_{m-a,\,static}$. The contour levels for all the maps are the same.

* The reason for two types of extinction model is simply as a result of the availability of the corresponding least-squares program. The two models of isotropic extinction are essentially the same.

* Lists of structure factors have been deposited with the British Library Document Supply Centre as Supplementary Publication No. SUP 71040 (4 pp.). Copies may be obtained through The Technical Editor, International Union of Crystallography, 5 Abbey Square, Chester CH1 2HU, England. [CIF reference: AS0627]

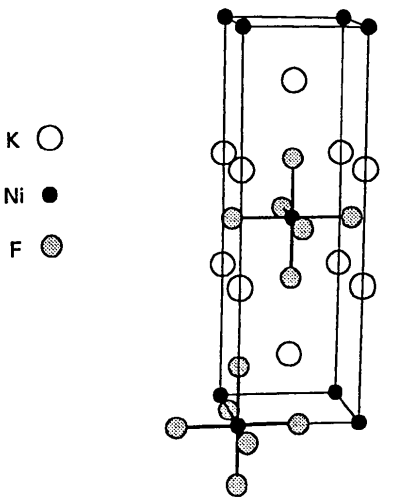

Fig. 1. Crystal structure of K_2NiF_4.

Table 2. *Agreement indices from the various refinements*

$R = \Sigma(F_o - F_c)/\Sigma F_o$, $wR = [\Sigma w(F_o - F_c)^2/\Sigma(wF_o^2)]^{1/2}$, $S = [\Sigma w(F_o - F_c)^2/(NR - NV)]^{1/2}$, where NV is the number of variables, NR is the number of reflections and g is the isotropic extinction coefficient.

	Conventional		Multipole (d^8)	
	Full data	High-order data	Monopole	Hexadecapole
$(\sin\theta/\lambda)$ (Å^{-1})	0–1.30	0.85–1.30	0–1.30	0–1.30
NV	13	12	18	29
NR	698	500	702	702
R	0.018	0.017	0.017	0.016
wR	0.02	0.02	0.018	0.016
S	6.09	2.76	5.35	4.96
$g \times 10^5$	1.35 (4)	1.35 (4)	0.97 (2)	0.96 (2)

Table 3. *Atomic parameters of* K_2NiF_4

(*a*) Full data refinement. (*b*) High-order [$(\sin\theta)/\lambda \geq 0.85$ Å^{-1}] refinement. (*c*) Multipole refinement. $u_{ij} \times 100$; $u_{12} = u_{13} = u_{23} = 0$.

		x	y	z	u_{11}	u_{22}	u_{33}
K	(*a*)	0	0	0.35377 (2)	1.628 (7)	u_{11}	1.214 (9)
	(*b*)	0	0	0.35388 (2)	1.618 (5)	u_{11}	1.214 (7)
	(*c*)	0	0	0.35380 (2)	1.625 (6)	u_{11}	1.204 (8)
Ni	(*a*)	0	0	0	0.672 (4)	u_{11}	0.834 (5)
	(*b*)	0	0	0	0.670 (4)	u_{11}	0.830 (4)
	(*c*)	0	0	0	0.650 (4)	u_{11}	0.811 (6)
F(1)	(*a*)	0	0.50	0	1.55 (3)	0.75 (2)	1.82 (3)
	(*b*)	0	0.50	0	1.56 (2)	0.75 (1)	1.78 (2)
	(*c*)	0	0.50	0	1.54 (3)	0.74 (2)	1.80 (4)
F(2)	(*a*)	0	0	0.15331 (7)	1.95 (2)	u_{11}	0.96 (2)
	(*b*)	0	0	0.15328 (6)	1.95 (2)	u_{11}	0.97 (1)
	(*c*)	0	0	0.1534 (1)	1.89 (2)	u_{11}	0.99 (3)

With these maps at four different projections of the unit cell, it is clear that we can correlate the aspherical density distribution around Ni atom with the *d*-orbital populations of Ni in a D_{4h} environment. These $\Delta\rho$ maps: (*a*) $\Delta\rho_{x-x}$, (*b*) $\Delta\rho_{m-a}$, (*c*) $\Delta\rho_{m-a,\text{ static}}$ of each plane are in good agreement around Ni, but excess density along Ni—F bond appears only in the experimental $\Delta\rho_{x-x}$ maps but not in the model density $\Delta\rho_{m-a}$ maps.

There is significant enhancement of the deformation density around Ni in the static maps (*c*), compared to the dynamic maps (*b*), as observed elsewhere (Wang, Yeh, Wu, Pai, Lee & Lin, 1991; Yeh & Wang, 1992). This may indicate that inclusion of extended high-order reflections enhances mainly the lone-pair electron density around the metal ion. The $\Delta\rho_{x-x}$ maps appear to have some deformation density along the Ni—F(1) bond on the xy plane but not on the Ni—F(2) bond. However, in the $\Delta\rho_{m-a}$ maps, no significant density was found along Ni—F bonds. Significant density appears only near the Ni atom. It is clearly shown (Figs. 2 and 3) that along all σ-bond directions ($d\sigma$), there is depletion of density. However, in the diagonal directions ($d\pi$) there is positive residual density along the pseudo-threefold axes direction ⟨113⟩, indicating a greater electron population on d_{xz}, d_{yz} orbitals (Figs. 4 and 5). These two maps are quite similar to that of K_2PtCl_6 (Takazawa, Ohba & Saito, 1990). According to simple crystal-field theory, if the Ni atom is at an O_h site, which is compatible with the Ni—F bond lengths, three $d\pi$ orbitals, d_{xz}, d_{yz} and d_{xy}, should be degenerate (t_{2g}) as in K_2PdCl_6 (Takazawa, Ohba & Saito, 1988), K_2PtCl_6 (Takazawa, Ohba & Saito, 1990), and $KNiF_3$ (Kijma, Tanaka & Marumo, 1983). However, in this work, the exact symmetry of the Ni atom is D_{4h} (4/*mmm*), which will cause the splitting of t_{2g} orbitals into e_g (d_{xz}, d_{yz}) and b_{2g} (d_{xy}) orbitals. Two $d\sigma$ orbitals (e_g) in O_h will also split into a_{1g} (d_{z^2}) and b_{1g} ($d_{x^2-y^2}$) orbitals. From the deformation-density distributions, the splitting of t_{2g} orbitals is obvious, where d_{xz}, d_{yz} orbitals (Figs. 4

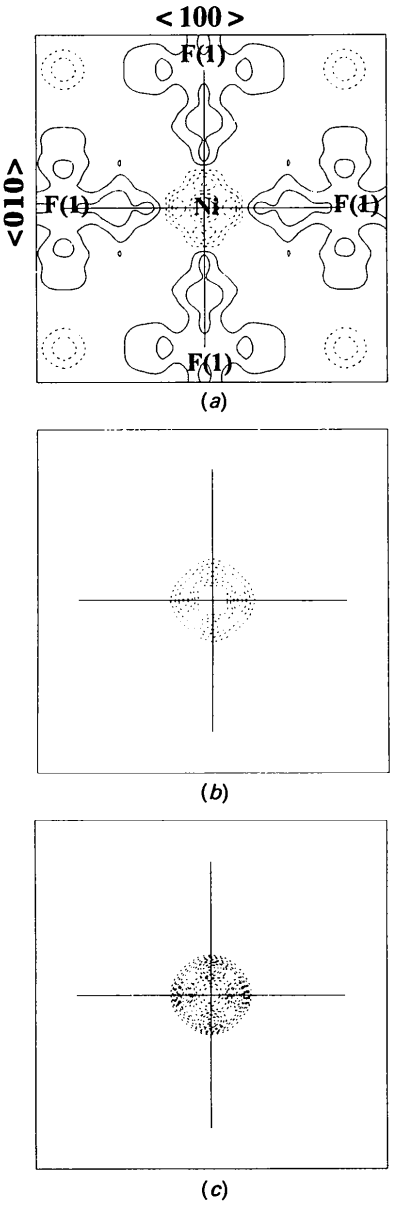

Fig. 2. Deformation-density maps of the *ab* plane: contour interval 0.2 e Å^{-3}; solid line = positive, dashed line = negative. (*a*) $\Delta\rho_{x-x}$, (*b*) $\Delta\rho_{m-a}$, (*c*) $\Delta\rho_{m-a,\text{ static}}$.

and 5) are apparently more populated than the d_{xy} orbital (Fig. 2). The *d*-orbital population derived from the multipole coefficients (Holladay, Leung & Coppens, 1983) according to D_{4h} symmetry are compared in Table 4 with those for K_2PdCl_6 (Takazawa, Ohba & Saito, 1988) and K_2PtCl_6 (Takazawa, Ohba & Saito, 1990).

The net charge on Ni is +0.28 (1) from the multipole refinement with d^8 and +1.82 (1) with d^{10} (see Table 4), so the total numbers of *d* electrons are roughly the same from both refinements. The populations among the five *d* orbitals are distributed more or less evenly with d_{xz}, d_{yz} most populated and d_{z^2} least populated. Although the *d*-orbital population indicates that the electron density around Ni is nearly spherical, the asphericity in deformation density around the Ni atom is still observable and conforms to the prediction of crystal-field theory. The peak density is indeed at the pseudo-threefold axis as in the true perovskite structures. The symmetry is lower than O_h as is apparent in the deformation density.

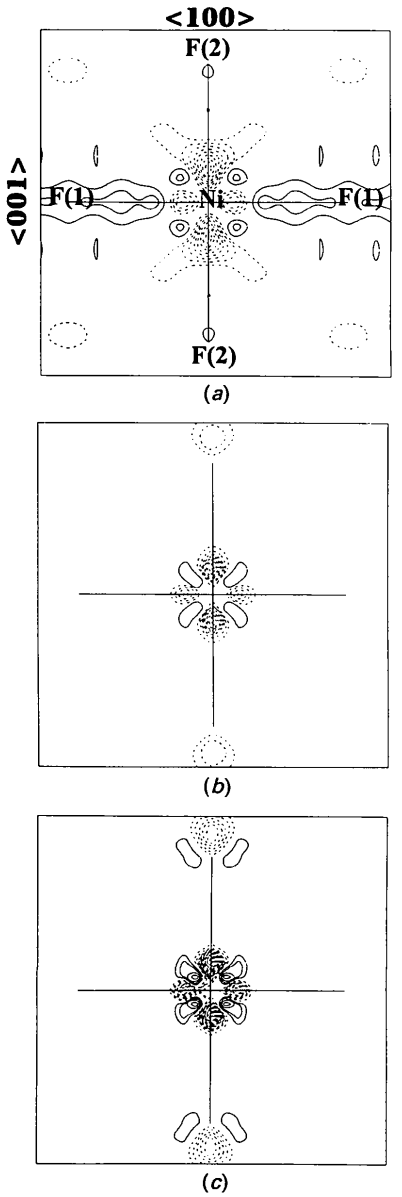

Fig. 3. Deformation-density maps of the *ac* plane: horizontal axis = ⟨100⟩, vertical axis = ⟨001⟩. (*a*), (*b*), (*c*) and contours are defined as in Fig. 2.

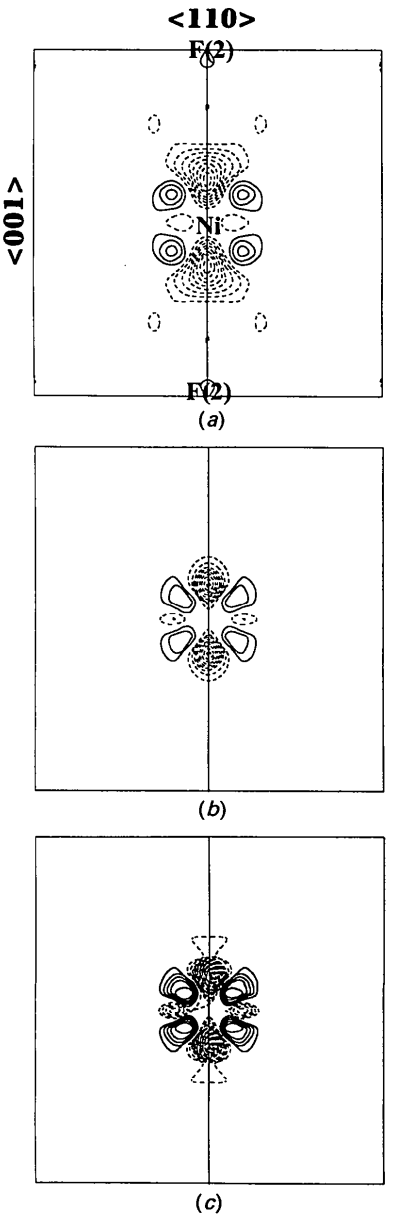

Fig. 4. Deformation-density maps of the plane at the bisection of the γ angle: ⟨110⟩ horizontal, ⟨001⟩ vertical. (*a*), (*b*), (*c*) and contours are defined as in Fig. 2.

Although the isotropic extinction coefficient obtained from the least-squares refinement is very small, 1.35×10^{-5}, the observed structure amplitudes for six reflections are corrected by more than 10%. Deformation-density distributions calculated without these reflections give no significant differences in the features of the deformation-density maps.

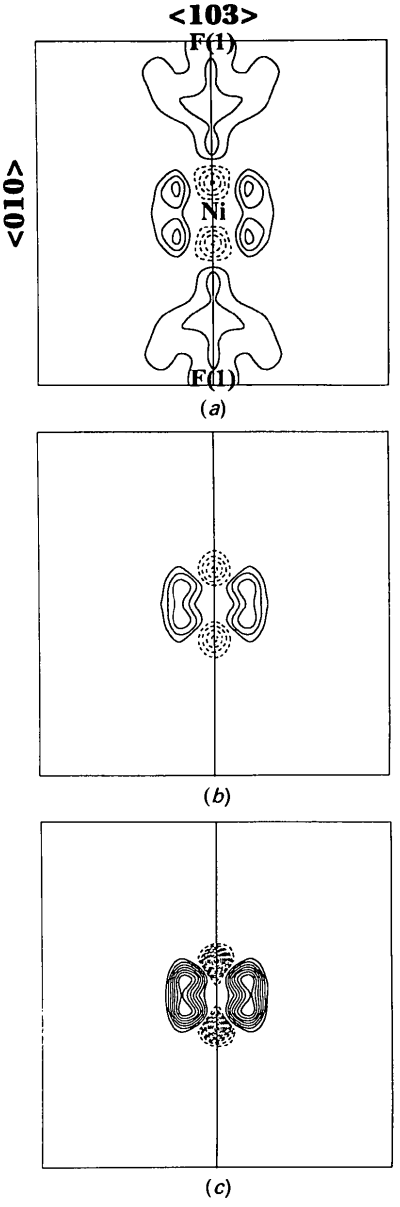

Fig. 5. Deformation-density maps of the plane at the bisection of the β angle: ⟨103⟩ horizontal, ⟨010⟩ vertical. (*a*), (*b*), (*c*) and contours are defined as in Fig. 2.

Table 4. *d-orbital populations of* Ni *from multipole refinements*

	K_2NiF_4		K_2PtCl_6*	K_2PdCl_6†
Space group	*I4/mmm*		*Fm3m*	*Fm3m*
Formal charge	+2		+4	+4
d configuration	d^{10}	d^8	d^{10}	d^{10}
κ	0.97 (1)	1.01 (1)	1.12 (3)	1.09 (2)
$d_{x^2-y^2}$, $b_{1g}(e_g)$	1.63 (1)	1.54 (1)	2.12 (12)	
d_{xy}, $b_{2g}(t_{2g})$	1.64 (1)	1.54 (1)	2.0	
d_{xz}, d_{yz}, $e_g(t_{2g})$	3.31 (1)	3.13 (1)	4.0	6.14 (8)
d_{z^2}, $a_{1g}(e_g)$	1.60 (1)	1.51 (1)	2.12 (12)	1.89 (7)
Total	8.18 (1)	7.72 (1)	8.12 (12)	8.03 (10)
Charge	+1.82 (1)	+0.28 (1)	+1.88 (12)	+1.97 (10)

* Takazawa, Ohba & Saito (1990).
† Takazawa, Ohba & Saito (1988).

We wish to thank Dr K. H. Lii at the Institute of Chemistry, Academia Sinica, Taipei, for preparation of the crystal. Financial support from the National Science Council of the Republic of China is appreciated.

References

ABDALIAN, A. T. & MOCH, P. (1978). *J. Appl. Phys.* **49**, 2189–2191.
ALCOCK, N. W. (1969). *Acta Cryst.* A**25**, 518–520.
BECKER, P. J. & COPPENS, P. (1974). *Acta Cryst.* A**30**, 129–147.
BIRGENEAU, R. J., GUGGENHEIM, H. J. & SHIRANE, G. (1969). *Phys. Rev. Lett.* **22**, 720–723.
GABE, E. J., LE PAGE, Y., CHARLAND, J.-P., LEE, F. L. & WHITE, P. S. (1989). *J. Appl. Cryst.* **22**, 384–387.
HANSEN, N. K. & COPPENS, P. (1978). *Acta Cryst.* A**34**, 909–921.
HOLLADAY, A., LEUNG, P. & COPPENS, P. (1983). *Acta Cryst.* A**39**, 377–387.
KIJMA, N., TANAKA, K. & MARUMO, F. (1983). *Acta Cryst.* B**39**, 557–561.
KOBLER, J., EYERT, V. & STICHT, J. (1988). *Physica C*, **153**, 1237–1238.
LARSON, A. C. (1970). *Crystallographic Computing*, edited by F. R. AHMED. Copenhagen: Munksgaard.
PISAREV, R. V., KARAMYAN, A. A., NESTEROVA, N. N. & SYRNIKOV, P. P. (1973). *Opt. Spectrosc.* **35**, 88–89.
PLUMIER, R. (1964). *J. Appl. Phys.* **35**, 950–951.
SAMOGGIA, G., PARMIGIANI, F. & LECCABUE, F. (1985). *Solid State Commun.* **55**, 157–158.
SINGH, K. K., GANGULY, P. & GOODENOUGH, J. B. (1984). *J. Solid State Chem.* **52**, 254–273.
STROBEL, K. & GEICK, R. (1982). *J. Phys. C*, **15**, 2105–2114.
TAKAZAWA, H., OHBA, S. & SAITO, Y. (1988). *Acta Cryst.* B**44**, 580–585.
TAKAZAWA, H., OHBA, S. & SAITO, Y. (1990). *Acta Cryst.* B**46**, 167–174.
VON BALZ, D. & PLIETH, K. (1955). *Z. Elektrochem.* **59**, 545–551.
VON RÜDORFF, W., KÄNDLER, J. & BABEL, D. (1962). *Z. Anorg. Allg. Chem.* **317**, 261–352.
WAGNER, G. & VON BALZ, D. (1952). *Z. Elektrochem.* **56**, 574–579.
WANG, Y., YEH, S. K., WU, S. Y., PAI, C. T., LEE, C. R. & LIN, K. J. (1991). *Acta Cryst.* B**47**, 298–303.
WANKLYN, B. M. (1975). *J. Mater. Sci.* **10**, 1487–1493.
YEH, S. K. & WANG, Y. (1992). *Acta Cryst.* B**48**, 319–324.